Electronic Supplementary Information for

Quantum anomalous Hall effect with high and tunable Chern number in monolayer NdN_2

Shengshi Li,[a‡] Xinyang Li,[b‡] Weixiao Ji,[a*] Ping Li,[a] Shishen Yan,[a] and Changwen Zhang[a*]

[a] *Spintronics Institute & School of Physics and Technology, University of Jinan, Jinan, Shandong, 250022, People's Republic of China. E-mail: hellojiweixiao@163.com; E-mail: ss_zhangchw@ujn.edu.cn*

[b] *School of Physics, Southeast University, Nanjing, Jiangsu, 211100, People's Republic of China.*

‡ *These authors contributed equally to this work.*

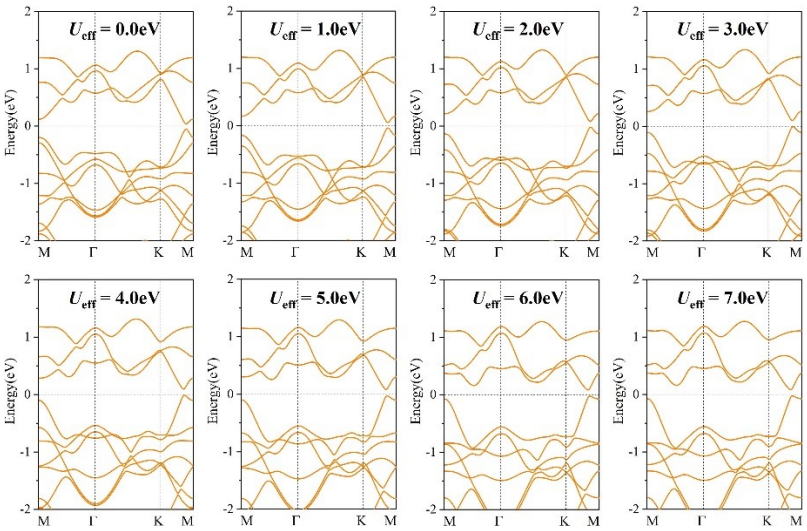

Fig. S1 Calculated SOC band structures of monolayer NdN_2 with different U_{eff}.

Table S1 Calculated lattice constant a, local magnetic moment of Nd atom $M_{Nd,}$ sum of local magnetic moment of two N atoms M_{N2}, and total magnetic moment per unit cell M_{tot} of monolayer NdN_2 using different pseudopotential for Nd atom.

	a (Å)	M_{Nd} (μ_B)	M_{N2} (μ_B)	M_{tot} (μ_B)
NdN_2 ($5s^25p^65d^16s^2$)	3.93	0.06	2.94	3.00
NdN_2 ($5s^26s^25p^65d^14f^3$)	3.92	0.13	2.87	3.00

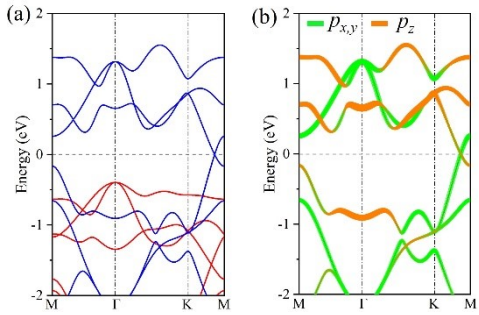

Fig. S2 Spin- and orbital-resolved band structures without SOC of monolayer NdN_2 obtained from GGA+*U* scheme with specific parameters of $U = 7.2$ eV and $J = 1.0$ eV implemented for the Nd-4*f* orbitals.

Table S2 Slater-Koster TB parameters for hexagonal lattice with lattice constant $a = 3.65$Å and interlayer distance $d = 1.77$Å. The unprimed and primed parameters correspond to nearest and next-nearest neighbor hoppings, respectively.

ϵ_s	ϵ_{p_x,p_y}	ϵ_{p_z}	$V_{ss\sigma}$	$V_{sp\sigma}$	$V_{pp\sigma}$	$V_{pp\pi}$	$V'_{pp\sigma}$	$V'_{pp\pi}$
-2.8	-2.39	-2.41	-0.15	-1.94	-1.90	-0.55	-0.6	-0.2

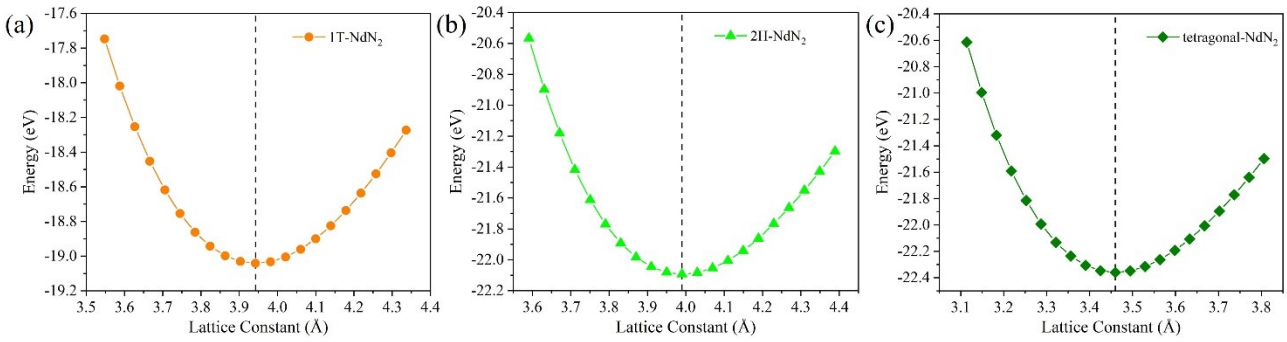

Fig. S3 Variation of energy as a function of lattice constant for monolayers 1T-NdN_2 (a), 2H-NdN_2 (b), and tetragonal-NdN_2 (c).

Part I: The MAE of monolayer NdN_2

Here, a detailed analysis is conducted on the magnetic anisotropy energy (MAE) of monolayer NdN_2. The angular dependence of MAE can be expressed as follows:

$$MAE(\theta,\varphi) = K_1 \cos^2\theta + K_2 \cos^4\theta + K_3 \cos^4\varphi$$

where K_1 and K_2 are anisotropy constants, while θ and φ are polar and azimuth angles in the spherical coordinates, respectively. By fitting the MAE results shown in Fig. S3(a), we can obtain the anisotropy constants, *i.e.*, K_1 = 143 μeV, K_2 = 35 μeV, and K_3 = 0 μeV. The positive value of K_1 indicates that monolayer NdN_2 exbibits an out-of-plane magnetic anisotropy with its easy magnetization axis along the *c* axis. While K_3 = 0 implies isotropic magnetization in the *xy* plane. Figure S3(b) displays a spherical plot of the MAE arising from magnetization rotation, in which the out-of-plane magnetization is more energetically favorable than the in-plane magnetization by 171 μeV/u.c..

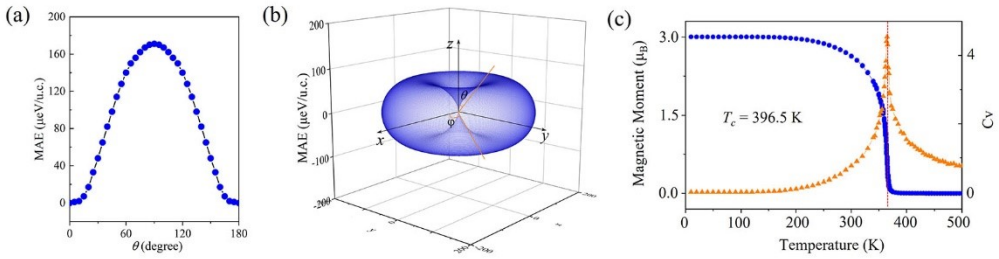

Fig. S4 (a) Polar angular dependence of MAE for monolayer NdN_2. (b) Magnetic anisotropy of NdN_2 through the whole space. (c) Variations of moment and C_v as a function of temperature.

Part II: The Curie temperature of monolayer NdN_2

Here, the Curie temperature (T_C) of monolayer NdN_2 is evaluated in detail. We first calculate exchange coupling parameters between nearest, next-nearest, and next-next-nearest neighbors (J_1, J_2, and J_3) using different magnetic configurations in relation to the Ising model:

$$H = -\sum_{i,j} J_1 M_i M_j - \sum_{k,l} J_2 M_k M_l - \sum_{m,n} J_3 M_m M_n \quad \text{(S2)}$$

where M is the net magnetic moment at the N site *i,* while (i,j), (k,l), and (m, n) run over the nearest, next-nearest and next-next-nearest N atoms. The obtained J_1 and J_2 are 8.4 meV and 1.4 meV, respectively. However, the value of J_3 is only 0.13 meV, which is negligible and can be disregarded. The T_C is estimated through Monte-Carlo (MC) simulation on a 200 × 200 supercell for 1×10^9 loops, based on the Ising Hamiltonian. Figure S3(c) presents the evolution of magnetic moment per unit cell with increasing temperature. It should be noted that the magnetic moment decreases to 0.0 μ_B when the temperature exceeds 396 K. Furthermore, we also calculate the heat capacity (C_v) expressed as:

$$C_v = \lim_{\Delta T \to 0} \frac{\Delta E_T}{\Delta T} \quad \text{(S3)}$$

where ΔE_T is the variation of total energy as the temperature increases from T to $T + \Delta T$. According to the simulated C_v curve shown in Fig. S3(c), it can be inferred that the 2D NdN_2 exhibits a T_C of 396.5 K, indicating its potential application

in spintronic devices operating at room temperature.

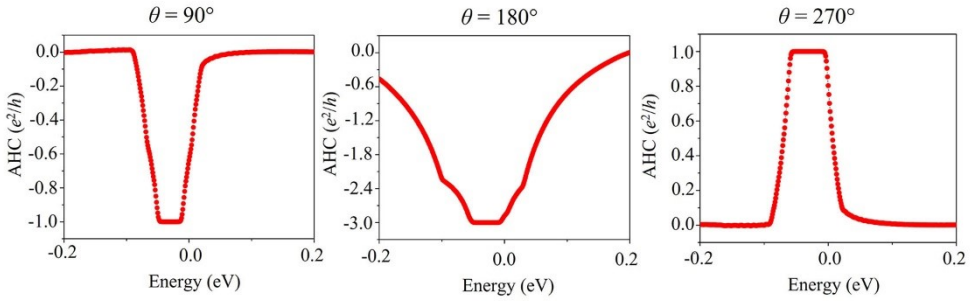

Fig. S5 Calculated AHC σ_{xy} as a function of Fermi level for the cases of $\theta = 90°$, $\theta = 180°$, and $\theta = 270°$, respectively. The corresponding Chern numbers are $C = -1$, $C = -3$, and $C = 1$.

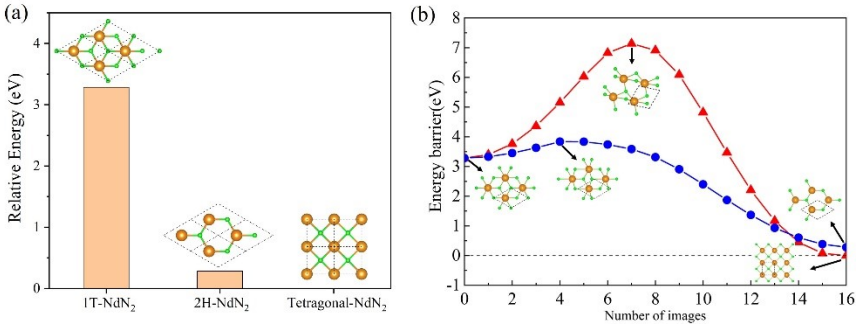

Fig. S6 (a) Relative energy of 2D allotropes of NdN_2. (b) Energy curve along the structural phase transition paths of 1T-2H and 1T-tetragonal predicted by the c-NEB method.

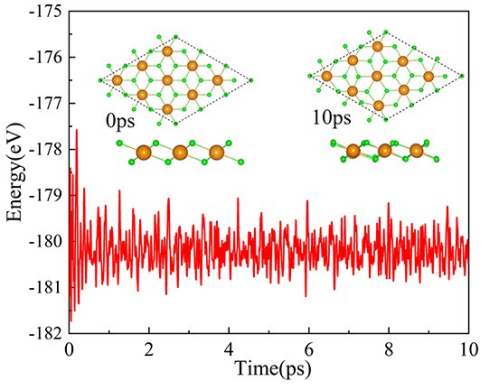

Fig. S7 Variation of total energy during 10ps AIMD simulation of monolayer 1T-NdN_2. Inserts show the initial and final structures of monolayer 1T-NdN_2 after 10ps at 300 K.

Table S3 The lattice constant *a*, bond length of Nd-N *d*, N-N distance along the *z* axis *h*, and total magnetic moment per unit cell M_{tot} of monolayer NdN_2 with 1T, 2H, and tetragonal phases.

	a (Å)	*d* (Å)	*h* (Å)	M_{tot} (μ_B)
1T-NdN_2	3.93	2.43	1.78	3.00
2H-NdN_2	3.99	2.41	1.70	0.15
Tetragonal-NdN_2	3.46	2.53	1.37	0.00

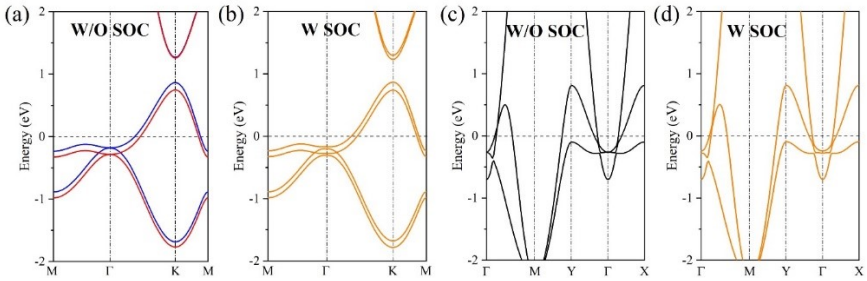

Fig. S8 Band structures of 1T-NdN_2 (a-b) and tetragonal-NdN_2 (c-d) monolayers without and with SOC. The red and blue lines represent the spin-up and spin-down states, respectively.